Investigation of the resonant behavior of point attachments on beams

B. Sawicki, A. Karlos, P. Paćko
AGH University of Science and Technology, Faculty of Mechanical Engineering and Robotics,
al. Mickiewicza 30, 30-059 Kraków, Poland
e-mail: **sawicki@agh.edu.pl**

Abstract

We consider the system of a beam with a scatterer attachment, where the scatterer can be of either of three types of mass-spring configuration. We explore the vibration response of the beam and the scatterer, aiming to identify special dynamical and scattering responses, for example a pinned point for the beam, full reflection or full transmission, and relate them to the dynamic properties of the scatterer, represented by its impedance. We observe that at the nominal resonance frequency(-ies) of the scatterer, the coupled system presents finite displacement. To further investigate this effect, the vibration response is compared to that of similar forced oscillators, but not attached to a beam, and the similarities and differences are illustrated. It is highlighted that resonances in the forced oscillators do not correspond to resonances in the corresponding systems with the scatterer on a beam. We also briefly discuss how the presence of the beam determines the absence of true resonances in lossless systems.

1 Introduction

Multiple scattering systems are frequently employed in metamaterials and acoustical devices for controlling and manipulating mechanical energy flow. In these systems, point-like or finite-size resonators and their dynamic characteristics are tuned and arranged in order to obtain a desired dynamic response of the structure [1]. Recently, re-configurability and tunability of these systems have been obtained by employing nonlinear properties of the scatterers [2].

The particular dynamic characteristics of multiple scattering systems depend on the impedance properties of the scatterers. For instance, a Vibration Neutralizer on a beam driven at its nominal resonant frequency corresponds to attaching an infinite impedance on the beam, and thus results in the anti-resonance of the beam-scatterer system, ideally creating a nodal point on the beam [3]. This and other specific vibrational behaviors of the attachments, and the related impedance conditions, link directly to the scattering properties of waves propagating in the substrate structure, that is, the beam. As a consequence, particular impedance values correspond to particular reflection and transmission coefficients. It is clear from the different impedance models that the scatterer structure determines its frequency characteristics, and the corresponding reflection and transmission properties [4]. In particular, certain structural models prohibit specific impedance values and, therefore, some values for the reflection coefficient, R, and the transmission coefficient, T, cannot be obtained. This is, for instance, the case for a mass attached to a beam through a spring, when one wants to obtain full transmission for a non-zero frequency.

The nonlinear properties of vibrating systems induce a number of phenomena that could be potentially used in multiple-scattering systems for manipulating wave propagation, e.g. amplitude dependency, energy redistribution to different frequency bands, bifurcations, chaos and other [5, 6, 7, 8]. These particular effects are typically associated with high vibration amplitudes and their analysis requires specific, application-dependent analytical and/or numerical tools. As a consequence, it is important to determine the amplitude vibration characteristics of the attachments and screen them for high-amplitude response bands or singular points.

In this work, we are interested in obtaining special dynamical responses, e.g. a pinned point for the beam, that can be related to specific impedance properties of the attached scatterer. For this purpose, we consider the system of an infinite beam with a single lossless point scatterer attached to it and investigate the vibration response of a number of different types of spring-mass models by relating specific scattering behaviors to particular values of the reflection and transmission coefficients. We then compare the responses of these scatterers coupled to a beam with structurally similar discrete-only systems in terms of their dynamic properties. The aim of this analysis is to discuss similarities and differences and identify frequencies at which these systems display a high amplitude response, that - if present - would be of importance for exploiting tunable nonlinear scattering properties.

2 Flexural wave scattering on a beam with a scatterer attached to it

The equation of motion for an Euler-Bernoulli beam with a point attachment located at $x = 0$, excited by an incident wave given by $a\mathrm{e}^{\mathrm{i}kx}$, is written as

$$d_x^4 w(x) - k^4 w(x) = \frac{\mu}{D} w(0)\delta(x), \tag{1}$$

where w_0 is the beam displacement, $k^4 = \omega^2\rho'/D$ is the flexural wavenumber, ω is the angular frequency, D is the bending stiffness, ρ' is the mass per unit length of the beam, μ is the scatterer impedance, defined as the ratio of the amplitude of the force acting from the scatterer to the beam at the point of attachment over the beam displacement amplitude, and $\delta(x)$ is the Dirac delta function. The dependence of the displacement on frequency is omitted from the notation for convenience. The solution of Equation (1) for the beam displacement is [4]

$$w = a\left(\mathrm{e}^{\mathrm{i}kx} + \frac{\mu g(x)}{1 - \mu g(0)}\right), \tag{2}$$

where $g(x) = (-\mathrm{e}^{\mathrm{i}k|x|} + \mathrm{i}\mathrm{e}^{-k|x|})/(4Dk^3)$. The beam displacement at the point of attachment, $w_0 = w(0)$, is of special interest, and follows from Equation (2) as

$$w_0 = \frac{a}{1 - \mu g_0}. \tag{3}$$

In the following we consider three (linear) undamped impedance models - labeled as *A*, *B* and *C* - given by

$$\begin{cases} \mu_A = m_1\omega^2 - \kappa_1, & (4) \\ \mu_B = \left(\dfrac{1}{m_1\omega^2} - \dfrac{1}{\kappa_1}\right)^{-1}, & (5) \\ \mu_C = -\kappa_1\left(\dfrac{1}{\hat{\omega}_1 - r_\kappa\left(\hat{\omega}_2^{-1} + 1\right)} + 1\right), & (6) \end{cases}$$

where m_α is (are) the scatterer mass(es), κ_α is (are) the scatterer spring stiffness(es), $\alpha = 1, 2$, $\hat{\omega}_\alpha = (\omega/\omega_{n\alpha})^2 - 1$, $\omega_{n\alpha} = \sqrt{\kappa_\alpha/m_\alpha}$, and $r_\kappa = \kappa_2/\kappa_1$. The formulas for models A and B are taken from [4], and that for model C is derived in Section 2.3. In the above, μ_A represents a mass (m_1) rigidly attached to a beam and connected to a rigid constraint via a spring (κ_1), μ_B represents a mass (m_1) connected to a beam through a spring (κ_1), and μ_C represents a two-Degree-of-Freedom (2DOF) scatterer, which comprises a mass (m_1) connected to a beam via a spring (κ_1) and a second mass (m_2) connected to the first via a second spring (κ_2). Schematics for each of the three impedance models are presented in Figures 1a-c, respectively.

The scattering response of the system with either of the three impedance models can be represented by the reflection, R, and transmission, T, coefficients, defined, respectively, as the ratio of the farfield reflected and transmitted beam displacement amplitude over the incident wave amplitude [4]. Limiting values of R and T include: full transmission, $|T| = 1$, $|R| = 0$, where the wave propagates through the substrate structure and is not altered by the presence of the scatterer, full reflection, $|T| = 0$, $|R| = 1$, where the wave cannot

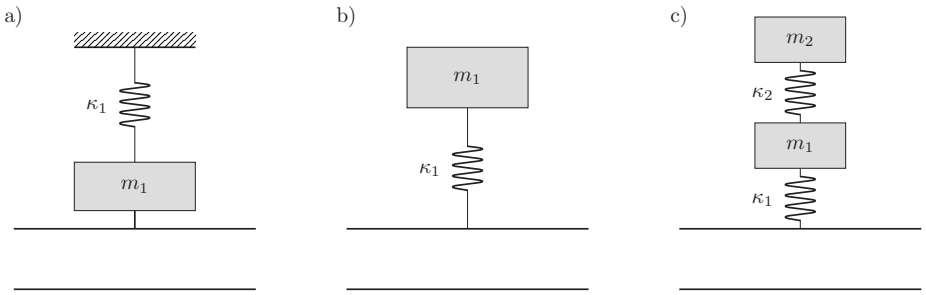

Figure 1: Schematics of the scatterer impedance models: (a) model A, (b) model B, (c) model C.

propagate through the structure and is reflected back at the point of attachment of the scatterer, and equal (lossless) energy partition, $|T| = |R| = \sqrt{2}/2$, where half of the incident wave energy is reflected and half is transmitted through the point of attachment of the scatterer. The reflection and transmission coefficients for a single scatterer located at $x = 0$ are given by [9]

$$R = \frac{\mathrm{i}\mu}{4Dk^3 - \mu\,(\mathrm{i} - 1)}, \qquad T = 1 + R. \tag{7}$$

From Equations (7) for the reflection and transmission coefficients and (3) for the beam displacement at the point of attachment, we can see that $R = 0 \Leftrightarrow T = 1 \Leftrightarrow \mu = 0 \Leftrightarrow w_0 = a$, and $T = 0 \Leftrightarrow R = -1 \Leftrightarrow \mu = -4Dk^3 \Leftrightarrow w_0 = -\mathrm{i}a$. Thus in the case of no reflection the incident wave simply passes unaffected through the attachment, while in the case of no transmission the incident wave is fully reflected with an inverted phase, and this is induced by a beam vibration of equal magnitude to that of the incident wave but with a phase difference of $-\pi/2$. Either of the impedance values $\mu = 0$ or $\mu = -4Dk^3$ results in $\mathrm{Im}\,(R) = 0$, while $\mu = 0$ additionally induces $\mathrm{Re}\,(R) = 0$. Other impedance values which give $|R| = 1$ or $|T| = 1$ also exist, but they are all active ($\mathrm{Im}\,(\mu) < 0$) and thus not considered here. Equal reflection and transmission, i.e. $|T| = |R| = \sqrt{2}/2$ for a lossless impedance, is obtained for $\mu = -2Dk^3$, which gives $R = -(1 + \mathrm{i})/2$ and $T = (1 - \mathrm{i})/2$.

In the following sections we investigate the specific scattering behaviors described above for the three defined impedance models and discuss the corresponding relation between the reflection and transmission coefficients, the scatterer impedance and the displacements of the various degrees of freedom in each model, the latter normalized by the incident wave amplitude. The parameter values used in the following analysis are $D = 1$ N m^2, $\rho' = 1$ kg/m, $m_1 = m_2 = 1$ kg, $\kappa_1 = \kappa_2 = 1$ N/m. The considered quantities are plotted against the ratio of the frequency to the scatterer's natural frequency. For some of the special scattering behaviors, determining the frequency ratio at which they occur requires the solution of fourth-order equations, a task which is not pursued here. In these cases, the corresponding frequencies are given indicatively for the particular parameter values used.

2.1 Model A

We start with the simplest among the considered impedance models, model A, whose impedance is plotted against the frequency ratio in Figure 2a, along with the moduli of the reflection and transmission coefficients. The moduli of the normalized displacement and of the reflection and transmission coefficients is plotted in Figure 2b, and the phases are plotted in Figure 2c. $|R|$ and $|T|$ are plotted in both Figures 2a and 2b for ease of comparison both with the impedance and with the displacement; the same format of plots is followed for models B and C. In model A, the scatterer is rigidly attached to the beam and therefore its displacement is identical to the beam displacement at the point of attachment, given in Equation (3). We consider three points of special interest along the direction of increasing frequency. The first characteristic point occurs at the limit of zero frequency, where the impedance has its minimum value, $\mu_A = -\kappa_1$, the displacement is equal to zero and the incident energy is equally reflected and transmitted. This frequency corresponds to DC excitation, where there is no wave propagation, and so is not treated further here. As frequency increases, there is a

frequency ratio for which the incident wave is fully reflected, which is observed here at $\omega/\omega_n \approx 0.36$, and where the displacement amplitude is equal in magnitude to the incident wave, $|w_0/a| = 1$, but with a relative phase $\angle(w_0/a) = -\pi/2$ rad, shown in Figure 2c. A second point of equal energy partition, apart from the DC case, occurs for $\mu_A = -2Dk^3$, which gives a frequency ratio of $\omega/\omega_n \approx 0.51$ for the parameter values used, where the displacement amplitude is maximum, $|w_0/a| = \sqrt{2}$. At the scatterer's natural frequency, $\omega/\omega_n = 1$, the impedance vanishes and the wave is fully transmitted ($|T| = 1$, $|R| = 0$, $w_0 = a$). At the high-frequency limit, $\omega/\omega_n \to \infty$, not visible in the plot, $|R|$ and $|T|$ asymptote to equal energy partition, and the displacement amplitude tends to zero, similarly to the the case of zero frequency. In the phase plots of Figure 2c it can be seen that there is a $-\pi$ rad phase jump in both the reflection and transmission coefficients when they are equal to zero, which corresponds to a phase inversion after passing through zero in the complex frequency plane. On the other hand, around the local maxima of these coefficients and of the displacement there is a smooth increase of the phase, more reminiscent of a damped resonance.

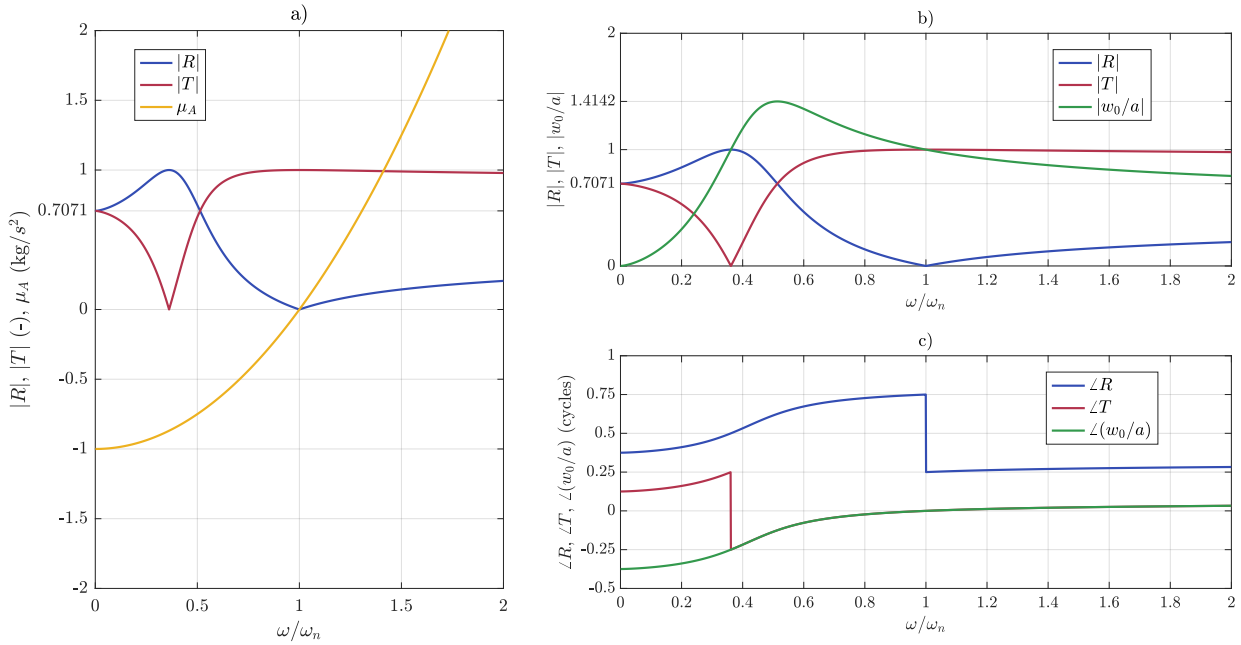

Figure 2: Impedance model A reflection and transmission coefficients, normalized displacement of the beam, modulus (upper) and phase angles (lower).

Overall, we observe that, although the scatterer is lossless, no singularity of infinite displacement occurs. For model A, where the mass is rigidly attached to the beam, the scatterer displacement singularity would induce movement of the whole beam. The investigation of possible displacement singularities becomes more interesting for models B and C, examined next, where there are additional degrees of freedom in the form of the scatterer mass(es).

2.2 Model B

We continue our analysis with model B, whose impedance is plotted against the frequency ratio in Figure 3a, along with the moduli of the reflection and transmission coefficients; the moduli and phases of the normalized displacement of the beam and the scatterer, as well as of R and T, are plotted in Figures 3b and 3c, respectively. In model B, the scatterer's mass m_1 is attached to the beam through a spring κ_1 and its displacement is given by [9]

$$w_1 = \frac{\kappa_1}{\kappa_1 - \omega^2 m_1} w_0, \tag{8}$$

where w_0 is given by Equation (3). Similarly to model A, we consider the points of special interest along increasing frequency ratio. Differently to model A, at the DC limit of zero frequency, $\omega/\omega_n \to 0$, $\mu_B = 0$,

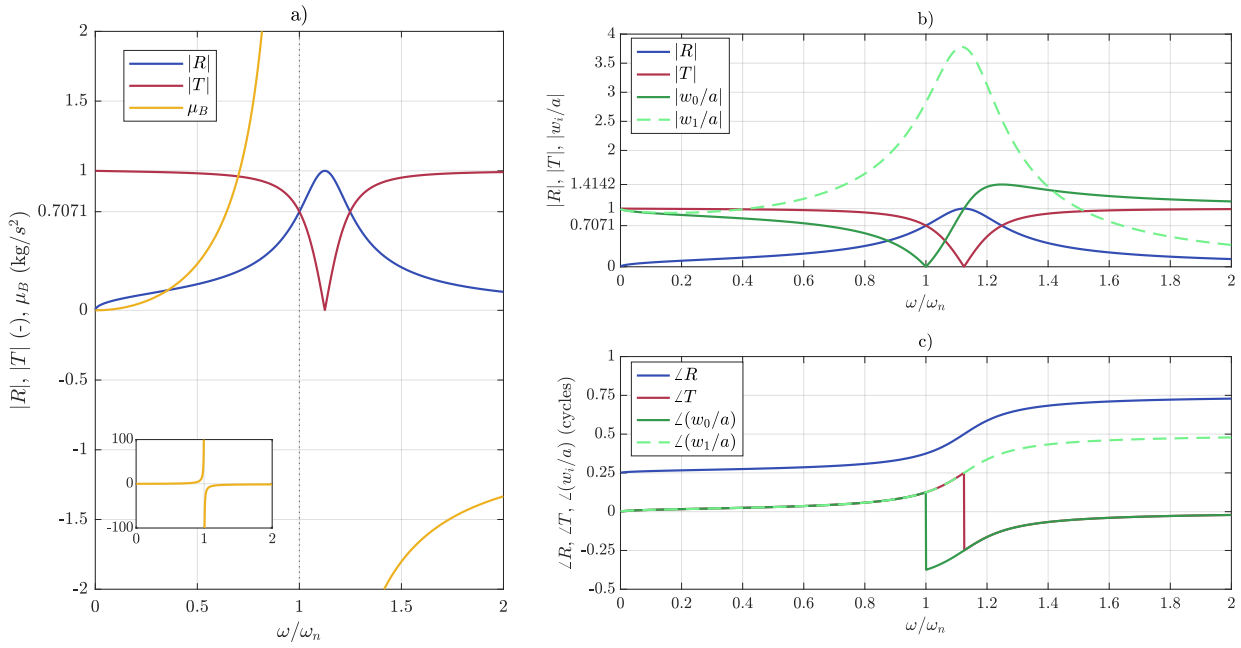

Figure 3: Impedance model B reflection, transmission coefficients and displacement of the beam, modulus (upper) and phase (lower).

which means that the impedance vanishes and the wave is fully transmitted ($|T| = 1, |R| = 0, w_0 = w_1 = a$). As frequency increases and approaches the scatterer's natural frequency, ω_n, the impedance μ_B tends to infinity, and at $\omega = \omega_n$ it jumps from $+\infty$ to $-\infty$. The absolutely infinite impedance imposes zero vertical beam displacement ($|w_0/a| = 0$), that is, the point of attachment on the beam is pinned, whereas the scatterer has a finite displacement ($|w_1/a| \approx 2.8$ for the parameter values used). In this case, $|R| = |T| = \sqrt{2}/2$ meaning that the incident energy is equally reflected and transmitted, where the transmitted part is due to the rotational motion of the beam [3], [10]. A second point of equal energy partition, apart from the DC case, occurs for $\mu_A = -2Dk^3$, at a frequency ratio of $\omega/\omega_n \approx 1.25$ for the parameter values used, where the displacement of the beam amplitude is maximum, $|w_0/a| = \sqrt{2}$. Between the two nontrivial, that is, excluding the DC, frequencies of equal energy partition, there exists a frequency for which the incident wave is totally reflected, $|R| = 1$ and $|T| = 0$, which is observed here at $\omega/\omega_n \approx 1.12$. At a slightly lower frequency, the displacement of the scatterer becomes maximum ($|w_1/a| \approx 3.7$), with relative phase, $\angle(w_1/a)$ slightly smaller than $\pi/2$. At the frequency of full reflection, the displacement of the beam is equal to the initial displacement of the incident wave ($|w_0/a| = 1$), but with a relative phase $\angle(w_0/a) = -\pi/2$ rad. Both characteristic features of the phase plots of model A, that is, the phase jump of $-\pi/2$ rad at the points of zero modulus and the smooth increase of the phase around a smooth peak of the modulus can be observed in the phase plots of Figure 3c at the respective points of the displacements and of R and T. It should be noted that contrary to the beam displacement, the mass displacement remains nonzero at all finite frequencies.

Overall, we again observe that although the scatterer is assumed to be lossless, no singularity, or infinite displacement, occurs, even when the scatterer is excited at its natural frequency. The scatterer's displacement curve, shown in Figure 3b, resembles that of a damped resonance and its peak is shifted from the natural frequency of the scatterer close to the frequency of full reflection phenomenon occurrence. Moreover, the displacement phase curve, shown in Figure 3c, does not exhibit any phase jumps related to the resonance but is smooth, as is the corresponding modulus peak. Instead, at the natural frequency of the scatterer, an antiresonance, that is, no displacement of the substrate structure (beam) is enforced, with a phase jump of $\angle(w_0/a) = -\pi/2$ rad.

2.3 Model C

The last scatterer model considered consists in a 2DOF scatterer, comprising two masses, m_1 and m_2, connected to each other with a stiffness, κ_2, with the first mass connected to the beam through a stiffness, κ_1, as shown in Figure 1c, which we call model C. The equations of motion of the masses are written as

$$-\omega^2 m_1 w_1 = \kappa_1(w_0 - w_1) + \kappa_2(w_2 - w_1), \tag{9a}$$

$$-\omega^2 m_2 w_2 = \kappa_2(w_1 - w_2), \tag{9b}$$

where w_0, w_1 and w_2 are the complex amplitudes of the displacements of the beam, the first mass and the second mass, respectively. Solving Equations (9) for w_1 and w_2 with respect to w_0 gives

$$w_1 = -\frac{w_0}{\hat{\omega}_1 - r_\kappa\left(\hat{\omega}_2^{-1} + 1\right)}, \tag{10a}$$

$$w_2 = -\hat{\omega}_2^{-1} w_1 = \frac{\hat{\omega}_2^{-1} w_0}{\hat{\omega}_1 - r_\kappa\left(\hat{\omega}_2^{-1} + 1\right)}, \tag{10b}$$

where $\hat{\omega}_\alpha = (\omega/\omega_{n\alpha})^2 - 1$, $\omega_{n\alpha} = \sqrt{\kappa_\alpha/m_\alpha}$, $n = 1, 2$, and $r_\kappa = \kappa_2/\kappa_1$. The scatterer impedance is defined as the force acting from the scatterer to the beam over the beam displacement amplitude at the point of attachment, that is, $\mu = f/w_0$. In the case of model C, the force is given by $f = \kappa_1(w_1 - w_0)$, so that using Equation (10a) gives the impedance as

$$\mu_C = -\kappa_1\left(\frac{1}{\hat{\omega}_1 - r_\kappa\left(\hat{\omega}_2^{-1} + 1\right)} + 1\right). \tag{11}$$

Once w_0 is calculated from Equation (3), the displacements of the scatterer masses can be calculated with Equations (10).

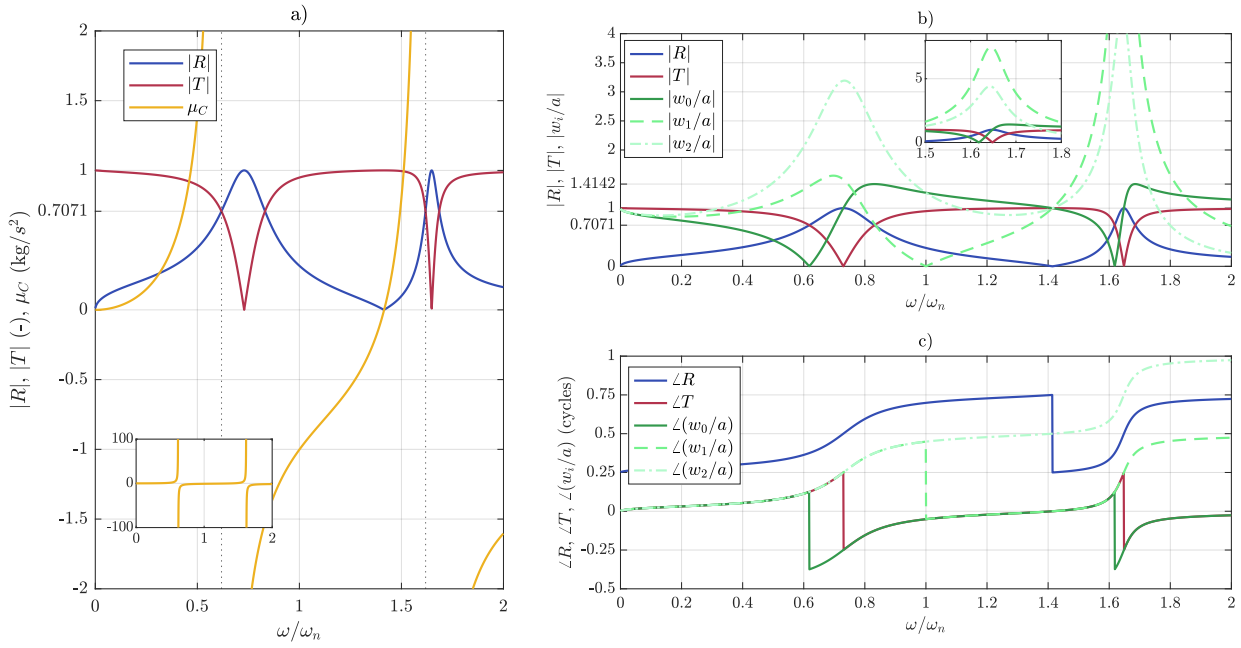

Figure 4: Impedance model C reflection and transmission coefficients, and displacements of the beam and the masses, modulus (upper) and phase (lower).

The impedance of model C is plotted against the frequency ratio in Figure 4a, along with the moduli of the reflection and transmission coefficients, and the moduli and phases of the normalized displacement of the

beam and the two scatterer masses are plotted in Figures 4b and 4c, respectively. It is noted that $\omega_{n1} = \omega_{n2} \equiv \omega_n$ for the parameter values used here. It can be noticed that in the case of no damping considered here, the impedance of model C can take both zero and infinite values, with the zero-crossing occurring between the two frequencies of absolutely infinite impedance. It can also be noticed that for frequency ratio $\omega/\omega_n \lessapprox 1$ the plots in Figures 4b and c are analogous to the corresponding plots of model B, presented in Figures 3b and c. Similarly to model B, at zero frequency the impedance is zero, so that the incident wave is fully transmitted ($|T| = 1, |R| = 0$), with the displacements of the beam (w_0) and the scatterer (w_1, w_2) being equal to the initial amplitude of the incident wave. Again, the next characteristic point occurs when the impedance $|\mu_C| = \infty$, here for $\omega/\omega_n \approx 0.6$, and corresponds to the $|T| = |R|$ condition, analogously to the $|\mu_B| = \infty$ case, with $|w_0/a| = 0$. The condition of equal reflection and transmission again occurs at $\omega/\omega_n \approx 0.82$, where $|w_0/a| = \sqrt{2}$ is at a local maximum, while $|w_1/a| \approx \sqrt{2}/2$ and $|w_2/a| \approx 2.5$. Similarly to the μ_B curves, the full reflection effect occurs between the two frequencies of $|T| = |R|$ and corresponds to relative beam displacement $|w_0/a| = 1$ and $|w_2/a| \approx 3.2$ at local maximum. The frequency ratio ω/ω_n where full reflection occurs, observed here at $\omega/\omega_n \approx 0.73$, depends on the material properties of the beam and the parameters of the scatterers. It is worth noting that neither the maximum normalized displacement of the lower nor of the upper scatterer mass are related to any of the considered characteristic points, although they both occur near the frequency of full reflection. Both displacement plots around this frequency present a peak that resembles a damped resonance.

All of these effects, analogous to model B, occur in the case of model C twice. As presented in Figure 4b, for the frequency ratio $\omega/\omega_n \in (1.4, 2)$, they appear in the same order as in $\omega/\omega_n \in (0, 1)$, as the impedance μ_C curve is similar in both sets. The significant difference is that the relative amplitude of the first scatterer is greater than the amplitude of the second, $|w_1/a| > |w_2/a|$, whereas in the first set of peaks, at lower frequencies, the opposite occurs, $|w_1/a| < |w_2/a|$.

Another interesting phenomenon occurs at the natural frequency of the scatterers, $\omega/\omega_n = 1$, where the impedance $\mu_C = -\kappa$ and the displacement of the first scatterer $|w_1/a| = 0$. Interestingly, the displacements of the beam and the second scatterer are equal, $|w_0/a| = |w_2/a|$, but with opposite phases (phase difference of $-\pi$ rad). Since the values of the stiffness for the two springs considered here are equal, the condition $w_0 = -w_2$ results in opposite spring forces acting on the first mass, m_1, which gives the observed antiresonance.

Similarly to the two previously discussed cases, we observe that although the scatterer is lossless, no infinite displacement occurs for any of its masses, even when the excitation frequency matches the natural frequency. Instead, the displacement curves, shown in Figure 4c, resemble a damped resonance shape at the two peaks for both scatterer masses. The impedance model C enforces an antiresonance of the substrate structure (beam) in two characteristic frequencies. Moreover, the displacement phase curve for mass m_2, shown in Figure 3c, does not exhibit any phase jumps, related to the resonance but is smooth, while the respective curve for mass m_1 does exhibit a phase jump at the point of the antiresonance of its displacement.

3 Comparison of a scatterer on a beam with discrete models

In this section we explore the behavior of the system of a scatterer attached to a beam and the impact of the scatterer's presence on propagating waves, and we investigate the relation of the system's efficiency in vibration neutralization with the natural frequency of the scatterer. Since we have assumed that the scatterer is either an SDOF model (for impedance models A and B) or a 2DOF model (for impedance model C), we look for analogies between the displacement characteristics of the scatterer on a beam and those for similar forced oscillators that are not attached to a beam.

3.1 Impedance model B vs SDOF

An SDOF system, consisting of a mass and a spring, can be placed on a rigid foundation, as illustrated in Figure 5a. When forced with a harmonic force of amplitude F_0, the equation of motion for the mass is

$$-\omega^2 m w_X + \kappa w_X = F_0, \tag{12}$$

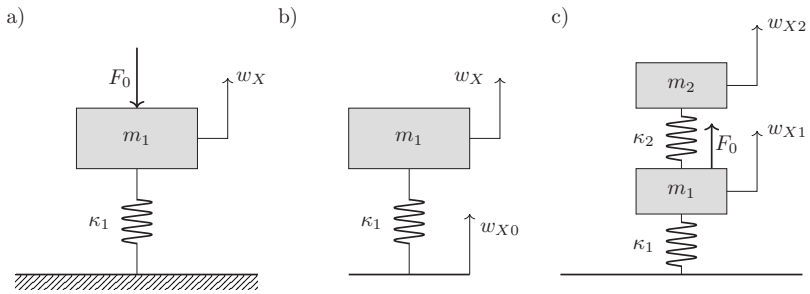

Figure 5: Schematic of a SDOF system excited with (a) an external force, (b) base excitation. (c) Schematic of a 2DOF system excited with an external force.

where w_X is the mass displacement. The solution of Equation (12) is

$$w_X = \frac{1}{1-\beta^2}\frac{F_0}{\omega_n^2 m}, \tag{13}$$

where $\beta = \omega/\omega_n$. Clearly, the response at the forcing frequency $\omega = \omega_n$, where $\omega_n = \sqrt{\kappa/m}$, becomes infinite. An SDOF system can also be excited with harmonic motion of the base, as illustrated in Figure 5b. In such a case, the governing equation of motion is

$$-\omega^2 m w_X + \kappa\left(w_X - w_{X0}\right) = 0, \tag{14}$$

where w_X describes the motion of the mass and w_{X0} describes the motion of the base. Solving Equation (14) gives the mass displacement as a function of the ground displacement as

$$w_X = \frac{1}{1-\beta^2} w_{X0}. \tag{15}$$

It can be seen that Equations (13) and (15) are equivalent under the condition $w_{X0} = F_0/\omega_n^2 m$, so that when the SDOF system is excited by base motion it again exhibits a resonance at its natural frequency, $\omega = \omega_n \Rightarrow \beta^2 = 1$, where the mass displacement w_X becomes infinite.

The normalized displacement, w_X/w_{X0}, of the SDOF oscillator and the normalized displacements of the scatterer and the beam for impedance model B are plotted in Figure 6a. As mentioned in Section 2.2, the lossless scatterer has a finite value of the displacement at its peak which can be compared to a damped resonance curve. In contrast, the displacement of the lossless SDOF oscillator is infinite, when the excitation frequency matches the natural frequency of the system. Moreover, the presence of the scatterer imposes an antiresonance for the beam at the natural frequency of the scatterer. From this comparison we can conclude that attaching a SDOF system on a beam changes the quality of its vibration response. The presence of the beam results in a finite response for the attached mass, similar to a damped resonance, which implies that the presence of the beam acts as a lossy element, or equivalently an energy sink, through the waves generated by the interaction of the incident wave with the scatterer.

3.2 Impedance model C vs 2DOF oscillator

In a 2DOF oscillator, the normalized amplitude of the main mass displacement is given by [11]

$$\frac{w_{X1}}{w_{st}} = \frac{p^2 - q^2}{\left(1-q^2\right)\left(p^2-q^2\right) - p^2 q^2 m_r}, \tag{16}$$

where $w_{st} = F_0/\kappa_1$, $p = \omega_{n_1}/\omega_{n_2}$, $q = \omega/\omega_{n_1}$, $m_r = m_2/m_1$, $\omega_{n1} = \sqrt{\kappa_1/m_1}$, $\omega_{n2} = \sqrt{\kappa_2/m_2}$, and the normalized amplitude of the second, auxiliary mass system is given by [11]

$$\frac{w_{X2}}{w_{st}} = \frac{p^2}{(1-q^2)\,(p^2-q^2) - p^2 q^2 m_r}. \tag{17}$$

The relative displacements of both of the masses in the 2DOF system and the relative displacements of the beam and the two masses in impedance model C are plotted in Figure 6b, where for both systems all masses and stiffnesses have the same values. It can be seen that for the undamped system of a 2DOF oscillator there exist two natural frequencies for which both of the masses m_1 and m_2 are in resonance - their relative displacements are infinite. Between these infinite peaks occurs an antiresonance, when the forcing frequency is equal to the natural frequency of an SDOF system consisting of a mass m_1 ($= m_2$) and a stiffness κ_1 ($= \kappa_2$). This means that the vertical motion of the main mass m_1 is constrained at its natural frequency in the absence of m_2, that is, its displacement amplitude is zero and thus does not vibrate at this frequency. In contrast, the relative displacement of the mass m_2 is never zero (for finite frequency) and is equal to the excitation displacement ($|w_{2X}/w_{st}| = 1$) at the frequency where the antiresonance of m_1 occurs.

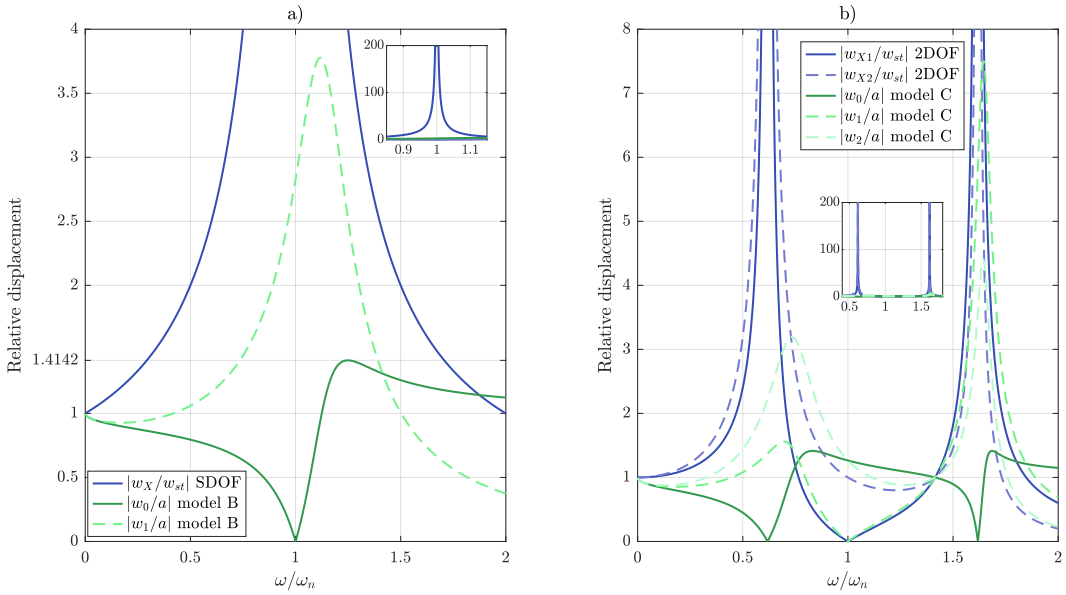

Figure 6: Comparison of (a) the relative displacement of an SDOF forced oscillator with the displacements of scatterer and beam in model B and (b) the relative displacements of the two masses in a 2DOF forced oscillator with the displacements of the two scatterer masses and the beam in model C.

On the other hand, it can be seen that for the scatterer of model C attached to a beam, there exist two frequency bands where both of the scatterer's masses m_1 and m_2 have a peak of vibration displacement. The main difference compared to the 2DOF oscillator is that these peak amplitudes are finite. There are three antiresonance points, two associated with zero displacement of the substrate structure (the beam) and coinciding with the natural frequencies of the isolated 2DOF system (blue solid curve), and one associated with natural frequency of either of the masses connected to the spring below them in isolation ($\omega_n = \sqrt{\kappa_1/m_1}$), resulting in zero displacement for the mass m_1. Interestingly, the displacement of the mass m_2 is never equal to zero for finite frequency. Similarly to model B, coupling the lossless 2DOF oscillator to a beam results in finite-amplitude vibration of both of the masses in the oscillator, and also results in antiresonance (zero displacement) points for both the substrate structure (the beam) and the lower mass (m_1). These effects again illustrate that the presence of the beam changes the quality of the vibration response of the attachment.

4 Conclusions

In this paper we presented three lossless scatterer models, consisting of mass(es) and stiffness(es), attached to a beam. The scattering of an incident flexural wave by these point scatterers is described by the reflection and transmission coefficients, which illustrate the capability of manipulation of the elastic wave propagation. We analyzed the scattering characteristics, along with the displacements of the discrete degrees of freedom of each model, in order to look for and describe characteristic points of full reflection ($|R| = 1$), full transmission ($T = 1$) or equal energy partition ($|R| = |T| = \sqrt{2}/2$). We found that the frequencies of occurrence of these characteristic points are in relation with the natural frequencies of the scatterer(s) in each of the models. Interestingly, we found that even though the scatterers considered are lossless, the displacement amplitudes of the vibrating masses have finite values. To investigate this effect further, we looked for analogies between the displacement characteristics of the masses of model B and model C and similar forced oscillators, SDOF and 2DOF, respectively, that are not attached to a beam. The results showed that by coupling the oscillator to a beam we obtain a finite value of the displacement of each of the components of the scatterer, even at its natural frequency when detached from the beam. This result may be important for systems with nonlinear scatterers [9], where the absence of true resonances, that is, exhibiting infinite (or, at least, high) displacement, may be of significance for their analysis and for exploiting their nonlinear properties.

Acknowledgements

The authors acknowledge support from the National Science Centre in Poland through Grant No. 2018/31/B/ST8/00753.

References

[1] P. Packo, A. N. Norris, and D. Torrent, "Metaclusters for the full control of mechanical waves," *Phys. Rev. Applied*, vol. 15, 2021.

[2] F. Quian and L. Zuo, "Tuned nonlinear spring-inerter-damper vibration absorber for beam vibration reduction based on the exact nonlinear dynamics model," *Journal of Sound and Vibration*, vol. 509, 2021.

[3] M. Brennan, "Control of flexural waves on a beam using a tunable vibration neutraliser," *Journal of Sound and Vibration*, vol. 222, no. 3, pp. 389–407, 1999. [Online]. Available: https://www.sciencedirect.com/science/article/pii/S0022460X98920314

[4] A. N. Norris and P. Packo, "Non-symmetric flexural wave scattering and one-way extreme absorption," *The Journal of the Acoustical Society of America*, vol. 146, no. 1, pp. 873–883, 2019. [Online]. Available: https://doi.org/10.1121/1.5087133

[5] Y.Starosvetsky and O.V.Gendelman, "Interaction of nonlinear energy sink with a two degrees of freedom linear system: Internal resonance," *Journal of Sound and Vibration*, vol. 329, 2010.

[6] G.Habib, T.Detroux, R.Viguié, and G.Kerschen, "Nonlinear generalization of den hartog's equal-peak method," *Mechanical Systems and Signal Processing*, vol. 52-53, 2015.

[7] T.Detroux, L.Renson, L.Masset, and G.Kerschen, "The harmonic balance method for bifurcation analysis of large-scale nonlinear mechanical systems," *Computer Methods in Applied Mechanics and Engineering*, vol. 296, 2015.

[8] K. J. Moore, J. Bunyan, S. Tawfick, O. V. Gendelman, S. Li, M. Leamy, and A. F. Vakakis, "Nonreciprocity in the dynamics of coupled oscillators with nonlinearity, asymmetry, and scale hierarchy," *Physical Review E*, vol. 97, 2018.

[9] A. Karlos, P. Packo, and A. N. Norris, "Nonlinear multiple scattering of flexural waves in elastic beams: Frequency conversion and non-reciprocal effects," *Journal of Sound and Vibration*, vol. 527, p. 116859, 2022. [Online]. Available: https://www.sciencedirect.com/science/article/pii/S0022460X22001043

[10] C. Yang and L. Cheng, "Suppression of bending waves in a beam using resonators with different separation lengths," *The Journal of the Acoustical Society of America*, vol. 139, pp. 2361–2371, 2016. [Online]. Available: https://dx.doi.org/10.1121/1.4947108

[11] M. J. Crocker, *Handbook of Noise and Vibration Theory*. Hoboken, New Jersey, USA: John Wiley and Sons, Inc., 2007.